American Mineralogist, Volume 72, pages 984–994, 1987

# $K_2Si_4O_9$: Energetics and vibrational spectra of glass, sheet silicate, and wadeite-type phases

KAREN L. GEISINGER
HP-ME-03-070-G6, Corning Glass Works, Corning, New York 14831, U.S.A.
NANCY L. ROSS
Geophysical Laboratory, Carnegie Institution of Washington, 2801 Upton Street, N.W., Washington, D.C. 20008, U.S.A.
PAUL MCMILLAN
Department of Chemistry, Arizona State University, Tempe, Arizona 85287, U.S.A.
ALEXANDRA NAVROTSKY
Department of Geological and Geophysical Sciences, Princeton University, Princeton, New Jersey 08544, U.S.A.

## ABSTRACT

Calorimetric experiments were performed on three phases of $K_2Si_4O_9$: a high-pressure phase with the wadeite structure containing both tetrahedrally and octahedrally coordinated Si, a low-pressure phase with a complex sheet structure containing solely tetrahedrally coordinated Si, and glass. The estimated enthalpy of fusion for the sheet-type phase is 42.9 $kJ \cdot mol^{-1}$, and the enthalpy of transition at 298 K for $K_2Si_4O_9$ (sheet-type phase) → $K_2Si_4O_9$ (wadeite-type phase) is $-31.7$ $kJ \cdot mol^{-1}$. Newly measured infrared and Raman spectra of each phase are presented. Vibrational models based on the spectra of the $K_2Si_4O_9$ polymorphs indicate that the entropy of transition at 298 K from the sheet-type phase to the wadeite-type phase is negative and in the range $-17$ to $-32$ $J \cdot K^{-1} \cdot mol^{-1}$. The data indicate that the wadeite-type phase is stable at low temperatures relative to the sheet-type phase. The calorimetric and vibrational calculations for the wadeite-type phase in this study are combined with existing thermochemical data to predict the phase boundary for the decomposition of K-feldspar to $K_2Si_4O_9$ (wadeite-type phase), $Al_2SiO_5$ (kyanite), and $SiO_2$ (coesite) with increasing pressure.

## INTRODUCTION

Goranson and Kracek (1932) noted that although the compound $K_2Si_4O_9$ is "unimportant geologically, . . . its abnormal behavior makes it unique among the silicates." They studied the low-pressure polymorphs of $K_2Si_4O_9$, which exhibit an inversion similar to that of $\alpha$–$\beta$ quartz at 865 K and atmospheric pressure. The compound melts at a low temperature for silicates, 1043 K at atmospheric pressure, and exhibits a negative $dP/dT$ for the melting curve. Thus, these crystalline phases are less dense than the liquid. Furthermore, the phases exhibit a very limited stability with pressure, disproportionating to $K_2Si_2O_5$ + $2SiO_2$ above, for example, ~0.125 GPa at ~950 K. A crystallographic study of the low-temperature phase demonstrates that the compound is structurally unique as well. It is based on a corrugated sheet of composition $[Si_8O_{18}]$, representing a condensation scheme of $SiO_4$ tetrahedra not observed for any other sheet silicate (Schweinsberg and Liebau, 1974).

A high-pressure investigation determined the existence of another polymorph of $K_2Si_4O_9$ with the wadeite ($K_2ZrSi_3O_9$) structure, based on three-membered rings of $SiO_4$ tetrahedra linked together by octahedrally coordinated Si (Kinomura et al., 1975; Swanson and Prewitt, 1983). This high-pressure phase is the only known example of a silicate containing both $^{IV}Si$ and $^{VI}Si$ linked across a bridging oxygen.

In this study, we examine the relative energetics of these sheet- and wadeite-type polymorphs of $K_2Si_4O_9$. Vibrational modeling based on Raman and infrared spectra provides estimates of heat capacities and entropies, and calorimetric techniques provide relative enthalpies. In addition, the new data for the wadeite-type phase are combined with literature data to give an estimate of the phase boundary for K-feldspar decomposition with pressure according to the reaction

$$\underset{\text{feldspar}}{2KAlSi_3O_8} \rightarrow \underset{\substack{\text{wadeite-type}\\ \text{phase}}}{K_2Si_4O_9} + \underset{\text{kyanite}}{Al_2SiO_5} + \underset{\text{coesite}}{SiO_2}.$$

This breakdown has been suggested as an intermediate step in the transition of feldspar to the hollandite-type structure (Kinomura et al., 1975).

0003–004X/87/0910–0984$02.00

## Experimental methods

### Synthesis

A sample of the high-pressure polymorph of $K_2Si_4O_9$ was provided by D. K. Swanson of SUNY Stony Brook. The sample was prepared from $K_2Si_4O_9$ glass (from the mixture $K_2CO_3$ + $4SiO_2$) held at 2.5 GPa and ~973 K for 24 h. The powder X-ray diffractometer pattern of the resultant material verified that this sample has the wadeite-type structure.

The bulk $K_2Si_4O_9$ glass used in this study was prepared from a stoichiometric mixture of dried reagent-grade $K_2CO_3$ and $SiO_2$ gel. The mixture was dry-ground in an agate mortar, placed in a covered Pt crucible, and decarbonated slowly over a 2-d period. The mixture was then held at ~1373 K for 24 h and finally quenched in air. The resulting glass was colorless and devoid of bubbles. Comparison of weights before and after melting indicated a weight loss of 0.24 wt%. Assuming the loss to be due to $K_2O$ volatilization alone, an appropriate amount of $K_2CO_3$ was added to the pulverized glass for correction (Kracek et al., 1929). This mixture was held at 1073 K for an additional 24 h and showed no significant weight loss other than that accounting for $CO_2$ volatilization. The resulting glass appeared optically homogeneous with a refractive index of 1.495 in agreement with that reported by Goranson and Kracek (1932).

A low-pressure polymorph was synthesized from this glass by repeatedly crushing and heating at 973–993 K over a 5-d period. The resulting crystals ($\leq 10$ $\mu$m) occurred invariably in polycrystalline aggregates similar to those described by Goranson and Kracek (1932). The powder X-ray pattern is consistent with that described by Schweinsberg and Liebau (1972).

### Spectroscopy

Raman spectra were obtained on 20–50-$\mu$m grains of sample using an Instruments S.A. U-1000 micro-Raman system. The 514.5-nm line of a Coherent Innova 90-4 Ar-ion laser was used for sample excitation. Spectral bandpass was 200 $\mu$m (1.8 $cm^{-1}$). Care was taken to eliminate laser parasite scattering in order to obtain clean spectra in the low-frequency region below 100 $cm^{-1}$, which is of importance for the vibrational modeling of thermodynamic properties (see below).

Powder infrared spectra were obtained from 1.0–1.5-mg samples in KBr (150 mg) discs on a Nicolet MX-1 Fourier-transform interferometer. Discs were heated in a vacuum oven for several hours to remove traces of adsorbed water. Preparations in the $K_2O$-$SiO_2$ system can be very hygroscopic and have a tendency to retain $CO_2$. Efforts to avoid these problems were undertaken by careful drying of reagents, synthesis, and storage conditions. Powder infrared spectra of all samples used in this study indicated no signficant adsorbed $H_2O$ or $CO_2$ or unreacted carbonate.

### Calorimetry

The calorimeter and basic calorimetric techniques used in this study have been reviewed previously (Navrotsky, 1977). Preliminary experiments indicated that the high-pressure wadeite-type phase transforms to a glass within 10 min at the calorimeter temperature (973 K). In order to measure the enthalpy of transformation, transposed-temperature-drop calorimetry was performed in which small samples (~30–40 mg) of the wadeite-type phase were sealed in Pt-foil capsules and dropped from room temperature (298 K) into the calorimeter at 973 K. The heat effect for each drop was measured over a period of approximately 45 min and the capsule retrieved and weighed. There was an average weight loss after dropping of ~1 wt%. Since this weight loss could not be characterized (e.g., from IR spectra as loss of $CO_2$ or $H_2O$), the weight loss was considered in the calculations only as a correction to the weight of the sample. The capsules were then dropped a second time into the calorimeter and the heat effect was measured again. The difference between the first and second drops represents the enthalpy of transformation of the wadeite-type phase to glass at 298 K and atmospheric pressure.

Enthalpies of solution in molten $2PbO \cdot B_2O_3$ at 973 K were measured on the remaining phases including the glass formed by transformation of the wadeite-type phase, the bulk synthetic glass, and the low-pressure sheet-type phase. The glass samples were crushed immediately before each solution experiment to avoid absorption of water or crystallization. Persistence of the glasses at 973 K was tested by equilibrating samples for 15–20 h in the calorimeter. Although the glasses fused to solid plates during equilibration (in fact they were supercooled liquids at calorimeter temperature), there was no evidence of crystallization from powder X-ray diffraction or microscopic observation. Therefore, standard solution calorimetric techniques were employed.

## Results and discussion

### Spectra

The vibrational spectra of the $K_2Si_4O_9$ polymorphs are as intriguing as their structural and energetic properties. Powder infrared and Raman spectra for the low- and high-pressure $K_2Si_4O_9$ polymorphs are shown in Figures 1a to 1d. There are no coincidences between the Raman and infrared spectra, as expected from the centric space groups ($P\bar{1}$ and $P6_3/m$ for the low- and high-pressure polymorphs, respectively: Schweinsberg and Liebau, 1974; Swanson and Prewitt, 1983). In micro-Raman spectroscopy, the low-pressure polymorph appeared as polycrystalline aggregates even under the highest magnification objective used (150×), and no polarization effects were observed in the Raman spectra. The high-pressure polymorph did show some variation in relative peak intensities on rotating the sample, suggesting that the aggregates contained single crystals on the scale of several micrometers.

The Raman spectrum for the low-pressure $K_2Si_4O_9$ polymorph (Fig. 1b) compares well with that obtained by Verweij and Konijnendijk (1976), although the present spectrum extends to lower wave number. This is important for the heat-capacity modeling discussed below. Verweij and Konijnendijk (1976) observed peaks at 1110 and near 500 $cm^{-1}$ not found in the present study: it is likely that these correspond to traces of $K_2Si_2O_5$ in their sample (see spectra of Verweij and Konijnendijk, 1976).

The structure of the low-pressure polymorph contains co-polymerized silicate tetrahedra with zero and one nonbridging oxygen (Schweinsberg and Liebau, 1972, 1974). A number of workers have found a strong Raman line near 1100 $cm^{-1}$ to be indicative of units of Si plus one nonbridging oxygen in a range of silicate glass and crystal compositions (Brawer and White, 1975; Verweij and Konihjnendijk, 1976; Mysen et al., 1982; Matson et al., 1983; McMillan, 1984). For example, crystalline $K_2Si_2O_5$ shows a strong Raman line at 1110 $cm^{-1}$ (Brawer and White,

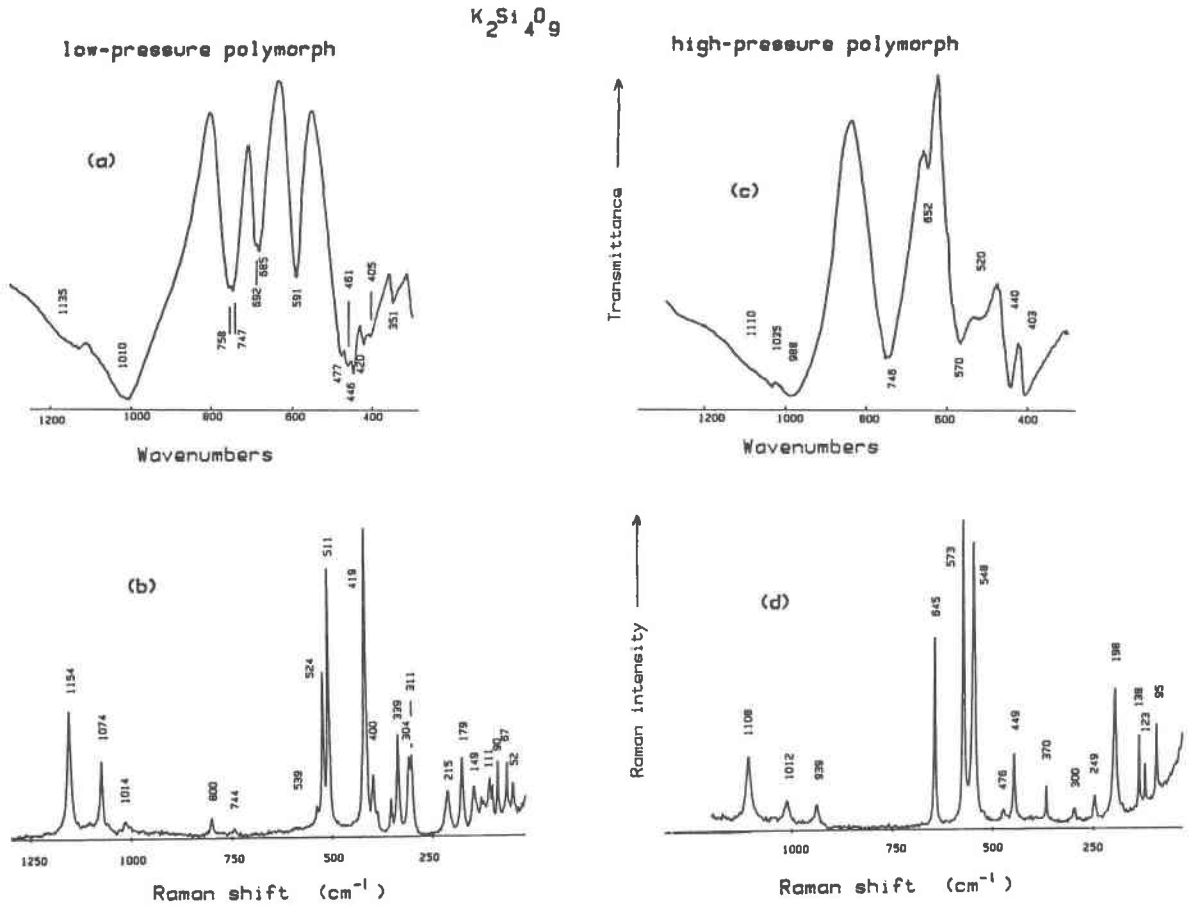


Fig. 1. (a) Infrared spectrum of low-pressure form of $K_2Si_4O_9$. (b) Raman spectrum of low-pressure form of $K_2Si_4O_9$. (c) Infrared spectrum of high-pressure (wadeite-type) form of $K_2Si_9O_9$. (d) Raman spectrum of high-pressure (wadeite-type) form of $K_2Si_4O_9$.

1975; Verweij and Konijnendijk, 1976). The Raman spectrum of low-pressure $K_2Si_4O_9$ shows no such feature: the major high-frequency lines occur at 1154 and 1074 $cm^{-1}$ (Fig. 1b). The reason for this is not clear: at present we do not feel confident in assigning these modes to any particular vibrations of the $K_2Si_4O_9$ lattice.

The strong sharp Raman modes in the 400–525-$cm^{-1}$ region (Fig. 1b) likely correspond to vibrations of bridging oxygens in the SiOSi linkages (McMillan, 1984; Matson et al., 1986). The low-pressure $K_2Si_4O_9$ structure contains four-membered rings of $SiO_4$ tetrahedra parallel to the *b* axis (Schweinsberg and Liebau, 1972, 1974). Sharma et al. (1981) observed the major Raman line of coesite, which also contains four-membered rings of $SiO_4$ tetrahedra, at 521 $cm^{-1}$. It is possible that one or both of the 524 and 511 $cm^{-1}$ peaks in the Raman spectrum of low-pressure $K_2Si_4O_9$ are due to a vibration of the bridging oxygens in the four-membered rings.

The infrared bands in the region of 600–750 $cm^{-1}$ (Fig. 1a) might also be assigned to vibrations associated with bridging oxygens in SiOSi linkages (Rutstein and White, 1971; Lazarev, 1972). However, the weak Raman modes near 750–800 $cm^{-1}$ and the infrared bands in the same region may also be associated with Si "cage" motions, which appear for highly polymerized silicates (Moenke, 1975; McMillan, 1984). For this reason, it is not possible to unambiguously assign the bands between 600 and 750 $cm^{-1}$ in the infrared spectrum of low-pressure $K_2Si_4O_9$.

The high-pressure (wadeite-type) polymorph of $K_2Si_4O_9$ shows a strong infrared band at 746 $cm^{-1}$ (Fig. 1c). The infrared spectrum of perovskite-type $MgSiO_3$, which contains $SiO_6$ octahedral groups sharing corners, shows a well-defined band at 797 $cm^{-1}$ (Weng et al., 1983; Williams et al., 1987). This band may be relatively unambiguously assigned to the asymmetric stretching vibration of the $SiO_6$ octahedra in the perovskite-type structure. This might suggest that the 746 $cm^{-1}$ band for $K_2Si_4O_9$ corresponds to the asymmetric stretch of the $SiO_6$ groups sharing corners with $SiO_4$ tetrahedra in the wadeite structure (Swanson and Prewitt, 1983). However, the wadeite structure also contains three-membered rings ($Si_3O_9$) of silicate tetrahedra. Lazarev (1962) has described a characteristic "ring band" near 750 $cm^{-1}$ in the infrared spectra of silicates containing $Si_3O_9$ rings, giving an alternate possible assignment for the 746-$cm^{-1}$ band of $K_2Si_4O_9$.

Similar alternatives exist for the interpretation of the

Raman bands of high-pressure $K_2Si_4O_9$ in the 550–650-$cm^{-1}$ region (Fig. 1d). As discussed above, this region corresponds to vibrations involving bridging oxygens in intertetrahedral SiOSi linkages, and it is possible that tetrahedral-octahedral SiOSi linkages may also vibrate in this region. However, Williams et al. (1987) have described a Raman peak near 500 $cm^{-1}$ for perovskite-type $MgSiO_3$ that may correspond to the symmetric stretching of $SiO_6$ groups in that structure. A similar assignment would be possible for one or more of the Raman bands near 500 $cm^{-1}$ for wadeite-type $K_2Si_4O_9$. Finally, Conjeaud and Boyer (1980) have observed a Raman line at 638 $cm^{-1}$ for pseudowollastonite ($CaSiO_3$ or $Ca_3Si_3O_9$), which contains three-membered rings of $SiO_4$ tetrahedra. It is possible that the 645-$cm^{-1}$ Raman peak of high-pressure $K_2Si_4O_9$ (Fig. 1d) also corresponds to the SiOSi vibrations within the three-membered rings of the wadeite-type structure.

In conclusion, there are no simple and unambiguous assignments for either the Raman- or the infrared-active vibrations for either the low- or high-pressure polymorph of $K_2Si_4O_9$, although some of the assignments are potentially important for the understanding of vibrational spectra of silicates. For example, the assignment of the high-frequency Raman peaks for the low-pressure polymorph will help in determining the degree of localization of Si–O stretching motions involving nonbridging oxygens, whereas the interpretation of the 500–750-$cm^{-1}$ region of the infrared and Raman spectra for the high-pressure polymorph will help separate contributions from SiOSi linkage vibrations and modes associated with stretching vibrations of $SiO_6$ octahedral groups. The actual assignment of infrared or Raman peaks to specific vibrations associated with structural units within the $K_2Si_4O_9$ polymorphs must await a detailed vibrational analysis of these structures. However, even without a detailed interpretation of the spectra of these phases, it is possible to use the infrared and Raman data to construct reasonable models for their vibrational density of states and to calculate useful estimates of their heat capacities and entropies as discussed in the next section.

## Vibrational modeling

Kieffer's lattice vibrational model (Kieffer, 1979a, 1979b, 1979c) was used to approximate the vibrational density of states of the sheet- and wadeite-type polymorphs of $K_2Si_4O_9$. The basic criterion for constructing vibrational models is that each model must be consistent with observed spectra and with acoustic and crystallographic data. Dispersion of the lowest-frequency optic mode is excluded in the present models since behavior of the optic branches across the Brillouin zone is unknown and cannot be described by simple diatomic chain analogies. Therefore, we consider dispersion to be, at present, an unknown and arbitrary adjustable parameter. The model treats each vibration as harmonic and predicts $C_V$, the heat capacity at constant volume. $C_V$ is converted to $C_P$ using the equation $C_P - C_V = TV\alpha^2K$ where $T$ is the temperature, $V$ is the molar volume, $\alpha$ is the thermal expansion coefficient, and $K$ is the bulk modulus. These parameters are presented in Table 6.

The low-pressure polymorph of $K_2Si_4O_9$ has $P\bar{1}$ symmetry and contains 30 atoms in its primitive unit cell. Three of the 90 vibrational degrees of freedom are acoustic modes. Acoustic velocities have not been measured for this phase, so velocities of 4.312 and 2.587 $km \cdot s^{-1}$ for the longitudinal- and shear-wave velocities, respectively, were estimated from Anderson's (1966) empirical equations. The corresponding, directionally averaged acoustic velocities (Kieffer, 1979a), 2.483, 2.711, and 4.312 $km \cdot s^{-1}$, characterize slopes of the acoustic branches at long wavelengths ($k = 0$). The acoustic branches follow a sinusoidal dispersion relation in Kieffer's model and reach 42, 46, and 73 $cm^{-1}$ at the Brillouin zone boundary.

The remaining 87 optic modes are distributed in a manner that is consistent with the vibrational spectra of the polymorph. The infrared and Raman spectra (Figs. 1a, 1b) define two distinct bands of frequencies. The first extends from 52 to 800 $cm^{-1}$ and the second extends from 1000 to 1150 $cm^{-1}$. The simplest vibrational models consistent with the spectra are presented in Figure 2. The vibrational density of states is approximated by an optic continuum encompassing the low-frequency modes and Einstein oscillators or by a second continuum spanning the high-frequency modes. The models differ according to how the modes are partitioned between the low- and high-frequency bands and how the high-frequency modes are modeled. Two approximations were used to estimate the fraction of modes at high frequencies. First, Kieffer's mode-partitioning method (Kieffer, 1979b, 1980) was applied to the low-pressure polymorph. The $[Si_8O_{18}]$ sheets in the structure can be described in terms of a $[Si_4O_{10}]$ "mica-like" sheet linked with fully polymerized $[Si_4O_8]$ units. The $[Si_4O_{10}]$ component has four bonds of the Si–O type and six bonds of the Si–O–Si type. The latter give rise to six symmetric and six antisymmetric stretching modes, whereas the former give rise to four stretching modes. The $[Si_4O_8]$ unit contains eight bonds of the Si–O–Si type that give rise to eight symmetric and eight antisymmetric stretching modes. Assuming that the Si–O vibrations and the antisymmetric Si–O–Si stretching modes lie at higher frequencies than the symmetric Si–O–Si stretching modes, 21% (18/87) of the optic modes is assigned to the modes lying between 1000 and 1150 $cm^{-1}$ (Figs. 2a, 2b). The second approximation is a simple proportionation scheme (Ross et al., 1986). The fraction of high-frequency modes is estimated by dividing the high-frequency range by the total-frequency range. In the present case, this fraction is $(1150 - 1000)/[(800 - 52) + (1150 - 1000)]$ or 16.7%. No assumptions are made about the types of modes present at high frequencies. Models incorporating this proportionation method are presented in Figures 2c and 2d.

Representation of the high-frequency modes as either Einstein oscillators or a continuum has little effect on $C_P$

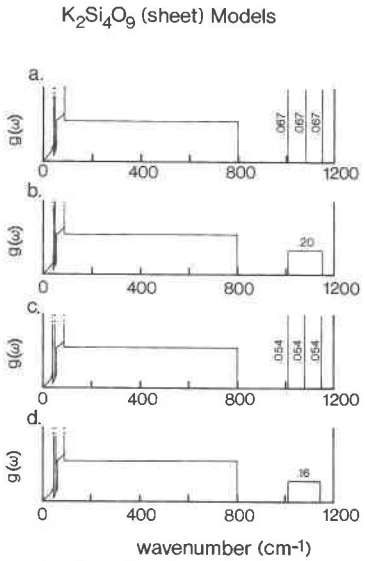


| | $C_p$ | $S^\circ$ |
|---|---|---|
| T(K) | (J/mol·K) | |
| 298 | 224.47 | 219.16 |
| 700 | 331.75 | 461.57 |
| 1000 | 354.76 | 584.83 |
| 298 | 224.51 | 219.32 |
| 700 | 331.75 | 461.74 |
| 1000 | 354.76 | 584.50 |
| 298 | 232.67 | 228.23 |
| 700 | 335.78 | 476.13 |
| 1000 | 357.19 | 600.02 |
| 298 | 232.48 | 228.17 |
| 700 | 335.45 | 475.83 |
| 1000 | 356.84 | 599.60 |

Fig. 2. Vibrational models for low-pressure polymorph of $K_2Si_4O_9$.

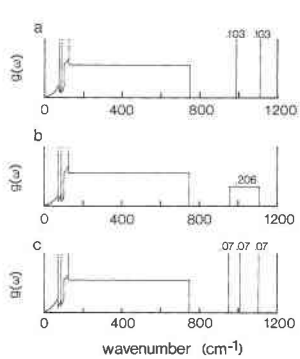


| T(K) | $C_p$(J/mol·K) | $S^\circ$ |
|---|---|---|
| 298 | 225.61 | 196.40 |
| 700 | 330.16 | 439.10 |
| 1000 | 350.89 | 560.90 |
| 298 | 226.56 | 196.70 |
| 700 | 331.09 | 440.37 |
| 1000 | 351.46 | 562.44 |
| 298 | 226.89 | 196.83 |
| 700 | 331.49 | 440.84 |
| 1000 | 351.85 | 563.05 |

Fig. 3. Vibrational models for high-pressure (wadeite-type) polymorph of $K_2Si_4O_9$.

and $S$ (compare Figs. 2a with 2b and 2c with 2d). The 4% decrease in the high-frequency optic modes, however, results in an increase of roughly 4% in $C_P$ and $S$ at 298 K (Fig. 2). This is due to the increase of modes in the low-frequency continuum. At 1000 K, $C_P$ and $S$ differ by less than 1% and 2.7%, respectively, for the two partitioning models.

The wadeite-type polymorph of $K_2Si_4O_9$ belongs to space group $P6_3/m$. Thirty atoms are contained in the primitive unit cell, and hence there are 90 vibrational degrees of freedom. Acoustic modes account for 3.3% of the total number of modes. Since sound-wave velocities have not been measured for this phase, longitudinal- and shear-wave velocities of 6.54 and 3.92 km·s$^{-1}$, respectively, were approximated with Anderson's (1966) empirical relations. The corresponding, directionally averaged velocities of 3.77, 4.11, and 6.54 km·s$^{-1}$ characterize three acoustic branches that are sinusoidally dispersed to 70, 76, and 122 cm$^{-1}$, respectively, at the Brillouin zone boundary.

The infrared and Raman spectra are used to model the distribution of the remaining 87 optic modes. The spectra show two distinct bands of frequencies. The first extends from 95 to 746 cm$^{-1}$ and the second from 939 to 1110 cm$^{-1}$ (Figs. 1c, 1d). The vibrational density of states is approximated with two optic continua (Fig. 3b) or a continuum with Einstein oscillators (Figs. 3a, 3c). Partitioning of optic modes into these two frequency regimes is approximated with Kieffer's method and with the proportionation method, as above. The wadeite structure has [$Si_3O_9$ rings.] Each ring has six bonds of Si–O type and three bonds of Si–O–Si type. The latter give rise to three symmetric and three antisymmetric stretching modes, and the former gives six stretching modes. Assuming that the Si–O and antisymmetric Si–O–Si vibrations lie at higher frequencies than the symmetric Si–O–Si vibrations, nine modes are assigned per [$Si_3O_9$] to the high-frequency band. There are two such units in the primitive unit cell of the high-pressure polymorph; thus the Kieffer method partitions 21% (18/87) of the optic modes to high frequencies. The proportionation method also predicts that 21% (171/822) of the optic modes lie at high frequencies. Heat capacities and entropies calculated from the vibrational models are within 1% of each other (Fig. 3). Modeling the high-frequency band modes with two Einstein oscillators, a continuum, or three oscillators has little effect on $C_P$ and $S$.

The vibrational models predict that the low-pressure polymorph of $K_2Si_4O_9$ has a significantly higher entropy than the high-pressure polymorph. Table 1 presents a comparison of entropies of transition, $\Delta S$, calculated from models approximating the vibrational density of states with (a) one continuum and three Einstein oscillators and (b) two continua. The calculated values of $\Delta S$ extend from $-16.7$ to $-32.2$ J·K$^{-1}$·mol$^{-1}$. Thus, despite uncertainties in the calculations, all models used predict that the entropy of transition has a significantly negative value. The high vibrational entropy of the sheet-type $K_2Si_4O_9$ is due to the population of optic modes at low frequencies that extend to 52 cm$^{-1}$, well below 95 cm$^{-1}$, the lowest-frequency optic mode observed in the wadeite-type polymorph. The calculated low-temperature heat capacities are shown in Figure 4. The heat capacity of the low-pressure polymorph below 200 K is notably larger than that of the high-pressure polymorph. At higher temperatures, the difference decreases because the modes at higher frequencies begin to make significant contributions to $C_P$.

## Calorimetry

Results of transposed-temperature-drop calorimetry on the wadeite-type phase are shown in Table 2. The observed heat effect for the first drop, 279.7 kJ·mol$^{-1}$, is associated with the following reaction:

$$\text{wadeite-type phase (298 K)} \rightarrow \text{liquid (973 K)}. \quad (1)$$

Strictly speaking, the product in Reaction 1 is a supercooled liquid as the calorimeter temperature lies above

TABLE 1. Comparison of entropies of transition for $K_2Si_4O_9$ (sheet-type → wadeite-type) from vibrational models with one continuum and three Einstein oscillators (2a, 2c, 3c) and two continua (2b, 2d, 3b)

| Models | | | |
|---|---|---|---|
| Sheet-type phase | Wadeite-type phase | $\Delta S^0_{298}$ ($J \cdot K^{-1} \cdot mol^{-1}$) | $\Delta S^0_{1000}$ ($J \cdot K^{-1} \cdot mol^{-1}$) |
| 2b | 3b | −21.13 | −17.07 |
| 2d | 3b | −29.87 | −32.18 |
| 2a | 3c | −20.84 | −16.32 |
| 2c | 3c | −29.92 | −32.01 |

the 752-K glass transition temperature (Richet and Bottinga, 1980). The observed heat effect for the second drop, 228.6 $kJ \cdot mol^{-1}$, is associated with the following reaction:

$$\text{glass (298 K)} \rightarrow \text{liquid (973 K)}. \quad (2)$$

This value is similar to the 973-K heat content of 235.2 $kJ \cdot mol^{-1}$ calculated from Richet and Bottinga's (1980) heat-capacity equations for glassy and liquid $K_2Si_4O_9$. Subtracting Reaction 2 from 1, we obtain

$$\text{wadeite-type phase (298 K)} \rightarrow \text{glass (298 K)}$$
$$\Delta H_{298} = 51.1 \pm 1.8 \text{ kJ} \cdot \text{mol}^{-1}. \quad (3)$$

Results of solution calorimetry on the glass formed by transformation of the wadeite-type phase ("transformed" glass) and the bulk glass are given in Table 3. Again, strictly speaking, under calorimetric conditions above $T_g$ these materials are supercooled liquids. Enthalpies of solution of these liquids are exothermic and are statistically identical at a conservative risk level of <1%, indicating that the wadeite-type phase transforms to a liquid that is energetically equivalent to the material formed by melting at 1 atm, at least when both are annealed in the calorimeter above $T_g$. The Raman spectra of both glasses are very similar to previously determined spectra of $K_2Si_4O_9$ glass prepared at 1 atm by quenching from the melt (see Fig. 5a) (Brawer and White, 1975; Verweij and Konijnendijk, 1976; Matson et al., 1983; Dickinson and Scarfe, 1985; Domine and Piriou, 1986). Given the great similarities between the calorimetric data and the spectra of the "transformed" and 1-atm glasses, we can combine the two data sets to better constrain the enthalpy of solution of $K_2Si_4O_9$ supercooled liquid at

$$\Delta H^{\text{liquid}}_{\text{soln,973}} = 21.8 \pm 0.5 \text{ kJ} \cdot \text{mol}^{-1}. \quad (4)$$

Results of solution calorimetry for the sheet-type phase are provided in Table 4. The enthalpy of solution is endothermic at

$$\Delta H^{\text{sheet-type phase}}_{\text{soln,973}} = 16.9 \pm 0.7 \text{ kJ} \cdot \text{mol}^{-1}. \quad (5)$$

Since the calorimeter temperature lies above the temperature of the reversible inversion (865 K) in the low-pressure polymorphs, Equation 5 represents the enthalpy of solution of the high-temperature, low-pressure form of $K_2Si_4O_9$ labeled $K_2Si_4O_9$-I by Goranson and Kracek (1932). For the purpose of our discussion, we will not

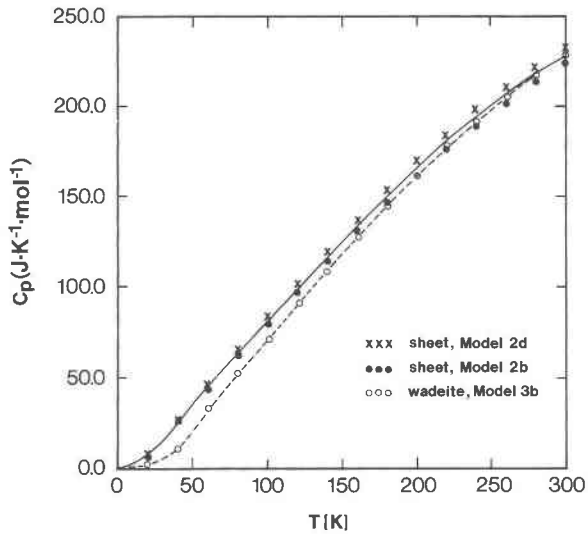


Fig. 4. Calculated low-temperature heat capacities of (a) low-pressure and (b) high-pressure forms of $K_2Si_4O_9$.

TABLE 2. Results of transposed-temperature-drop calorimetry on high-pressure wadeite-type phase

| | $\Delta H$ (first drop) ($kJ \cdot mol^{-1}$) | $\Delta H$ (second drop) ($kJ \cdot mol^{-1}$) |
|---|---|---|
| | 278.31 | 228.15 |
| | 274.40 | 229.89 |
| | 280.78 | 230.58 |
| | 278.83 | 224.64 |
| | 280.07 | 231.40 |
| | 285.59 | 227.07 |
| Mean | 279.66 ± 1.49 | 228.62 ± 1.03 |

*Note:* Error represents one standard deviation of the mean.

TABLE 3. Enthalpies of solution of "transformed" and bulk glasses in $2PbO \cdot B_2O_3$ at 973 K

| "Transformed" glass | | Bulk glass | |
|---|---|---|---|
| Sample weight (mg) | $\Delta H_{973}$ ($kJ \cdot mol^{-1}$) | Sample weight (mg) | $\Delta H_{973}$ ($kJ \cdot mol^{-1}$) |
| 26.09 | −22.82 | 32.57 | −19.53 |
| 28.71 | −18.93 | 25.29 | −21.00 |
| 27.56 | −20.04 | 26.08 | −22.95 |
| 25.48 | −24.76 | 30.47 | −23.90 |
| 28.51 | −21.66 | 27.25 | −22.96 |
| | | 33.53 | −21.05 |
| | | 26.62 | −22.34 |
| | | 26.79 | −23.51 |
| | | 26.48 | −19.69 |
| Mean (transformed) = −21.64 ± 1.03 | | | |
| Mean (bulk) = −21.88 ± 0.54 | | | |
| Mean (all) = −21.79 ± 0.48 | | | |

*Note:* Error represents one standard deviation of mean.

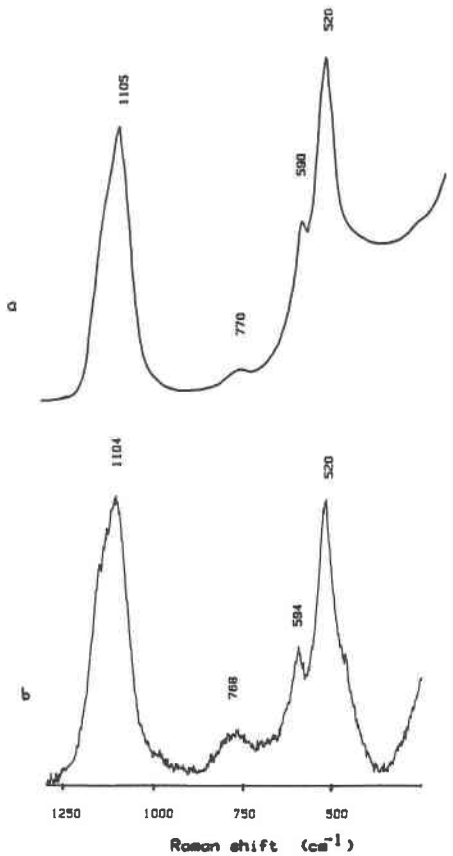


Fig. 5. Raman spectra of (a) $K_2Si_4O_9$ glass reported by melting at 1 atm (provided by J. Dickinson) and (b) glass obtained by transformation of high-pressure (wadeite-type) form on heating to 973 K.

distinguish between these high- and low-temperature sheet-type polymorphs. The differences in their thermochemical properties are small when compared to the wadeite-type polymorph. Actual $\Delta H$ and $\Delta S$ values for the low–high inversion at 865 K given by Goranson and Kracek (1932) are 3.2 ± 0.4 kJ·mol$^{-1}$ and 3.8 kJ·mol$^{-1}$·K$^{-1}$, respectively.

Combining the enthalpy of solution data for the glass and sheet-type phase (Eqs. 4 and 5), we estimate the enthalpy of the following reaction:

$$\text{sheet-type phase (973 K)} \rightarrow \text{liquid (973 K)}$$
$$\Delta H_{973} = 16.9 - (-21.8) = 38.7 \pm 0.9 \text{ kJ·mol}^{-1}. \quad (6)$$

Given the experimental heat-capacity data for glassy and liquid $K_2Si_4O_9$ (Richet and Bottinga, 1980) and some estimate of the heat capacity for the sheet-type phase, one can estimate the heat of fusion at $T_f$ = 1043 K from Equation 6. Experimental heat-capacity data are not available for the sheet-type phase. However, Eliezer et al. (1978) have estimated a heat-capacity equation for crystalline $K_2Si_4O_9$ generally valid above 1000 K. Combining these data yields

$$\Delta H_{\text{fusion},1043} = 38.7 + 4.3 = 43.0 \text{ kJ·mol}^{-1}. \quad (7)$$

TABLE 4. Enthalpies of solution of low pressure sheet-type phase in $2PbO \cdot B_2O_3$ at 973 K

| Sample weight (mg) | $\Delta H_{973}$ (kJ·mol$^{-1}$) |
|---|---|
| 23.19 | 16.81 |
| 22.59 | 13.49 |
| 26.06 | 20.78 |
| 25.68 | 19.39 |
| 31.78 | 18.17 |
| 31.25 | 13.36 |
| 29.71 | 15.79 |
| 35.89 | 18.89 |
| 42.58 | 16.05 |
| 40.42 | 13.70 |
| 35.13 | 19.92 |
| 40.90 | 16.34 |
| Mean | 16.91 ± 0.74 |

*Note:* Error represents one standard deviation of mean.

This enthalpy of fusion lies within the error of the experimental determination of Goranson and Kracek (1932) of 49.0 ± 9.8 kJ·mol$^{-1}$. Note that an enthalpy of fusion (43.2 kJ·mol$^{-1}$) calculated using the vibrationally modeled heat capacity is in excellent agreement with the estimate in Equation 7, suggesting that the thermal expansion and compressibility estimates for the sheet-type phase are not unreasonable for high temperatures.

Finally, we estimate the enthalpy of transformation of the sheet-type phase to the wadeite-type phase by combining Equations 3 and 6.

$$\text{sheet-type phase} \rightarrow \text{wadeite-type phase}$$
$$\Delta H = 38.7 - 51.1 = -12.4 \text{ kJ·mol}^{-1}. \quad (8)$$

A better estimate at 298 K of the sheet → wadeite transformation requires a measurement of Reaction 6 at 298 K. Kracek et al. (1953) determined this $\Delta H_{298}$ (sheet-type phase → glass) = 19.3 kJ·mol$^{-1}$ by hydrofluoric acid solution calorimetry. We estimate an error on the order of ±3.8 kJ·mol$^{-1}$ based on the reported errors of Kracek et al. (1953) on directly determined heats of solution. This $\Delta H_{298}$ is significantly different from the corresponding 973-K value (Eq. 6), indicating a pronounced difference in the heat capacity of $K_2Si_4O_9$ glass and supercooled liquid, which is borne out by calorimetric data near $T_g$ = 752 K of Richet and Bottinga (1980). The data at 298 K (Kracek et al., 1953) and at 973 K (this study) are consistent with each other. Assuming that the heat capacities of the sheet-type phase and glass are quite similar below $T_g$ and crystal and supercooled liquid differ by a roughly constant amount (equal to the difference at $T_g$) above $T_g$, one estimates $\Delta H_{973}$ (sheet-type → liquid) = 37.7 kJ·mol$^{-1}$ starting from the $\Delta H_{298}$ value of Kracek et al. (1953). Considering the assumptions, this is in remarkably good agreeement with the new experimental value from this study of 38.7 kJ·mol$^{-1}$.

Combining the Kracek et al. (1953) data with Equation 3 yields

$$\text{sheet-type phase (298 K)} \rightarrow \text{wadeite-type phase (298 K)}$$
$$\Delta H_{298} = 19.3 - 51.0 = -31.7 (\pm 4.2) \text{ kJ·mol}^{-1}. \quad (9)$$

TABLE 5. Heats of formation and standard entropies of phases involved in K-feldspar decomposition (Eq. 10)

| Phase | $\Delta H_{f,298}$* (kJ·mol$^{-1}$) | $S^0_{298}$** (J·K$^{-1}$·mol$^{-1}$) |
|---|---|---|
| $KAlSi_3O_8$ (sanidine) | −216.15 ± 1.97 | 232.80 ± 0.48 |
| $K_2Si_4O_9$ (wadeite-type) | −314.08 ± 3.66 | 198.93 ± 3.98 |
| $Al_2SiO_5$ (kyanite) | −5.33 ± 0.96 | 83.76 ± 0.39 |
| $SiO_2$ (coesite) | 2.93 ± 0.29 | 38.53 ± 0.86 |

* Heat of formation from oxides; all data from Robie et al. (1978) except $K_2Si_4O_9$ (see text) and coesite (Akaogi and Navrotsky, 1984).
** Data from Robie et al. (1978) except $K_2Si_4O_9$ (this study) and coesite (Akaogi and Navrotsky, 1984).

Equation 9 indicates that the transformation of the sheet- to the wadeite-type phase remains strongly exothermic when heat-capacity differences are included.

Insufficient data for the low-pressure sheet phases preclude any absolute determination of heat capacity and entropy, particularly at low temperature, and thus any reliable calculation of phase equilibria for the $K_2Si_4O_9$ polymorphs. The negative enthalpy of transformation from the sheet- to the wadeite-type phase at 298 K (Eq. 9) and the large negative entropy of transformation suggested from vibrational calculations together imply that the wadeite structure is the stable phase as $T \rightarrow 0$ K. However, kinetic hindrances almost certainly preclude experimental verification of this.

### Breakdown of K-feldspar with pressure

Kinomura et al. (1975) have suggested that the breakdown of potassium feldspar with pressure,

$$\underset{\text{(feldspar)}}{2KAlSi_3O_8} = \underset{\text{(wadeite-type)}}{K_2Si_4O_9} + \underset{\text{(kyanite)}}{Al_2SiO_5} + \underset{\text{(coesite)}}{SiO_2} \qquad (10)$$

is an intermediate step in the transition of feldspar to the hollandite-type structure. We have estimated the phase boundary of this reaction by combining the calorimetric and vibrational data presented above for wadeite-type $K_2Si_4O_9$ with the existing thermochemical data for K-feldspar, kyanite, and coesite. The condition for equilibrium in a closed system at constant pressure and temperature is

$$\Delta G_{T,P} = 0, \qquad (11)$$

where

$$\Delta G_{T,P} = \Delta H^0_T - T\Delta S^0_T + \int_{1\text{ atm}}^{P} (\Delta V_{T,P})\, dP. \qquad (12)$$

The last term was estimated using a modified Birch-Murnaghan equation,

$$V_{T,P} = V^0_{298}\,[1 + \alpha\,(T - 298)]\,[PK'/(K + 1)]^{-1/K}, \qquad (13)$$

where $V^0_{298}$, $\alpha$, $K$, and $K'$ are the molar volume at 298 K, the thermal-expansion coefficient, the bulk modulus, and its pressure derivative, respectively (Navrotsky et al., 1979). $\Delta H^0_{298}$ of the reaction determined from the heats of formation of the phases at 298 K (Table 5) is 72.6 ± 5.5 kJ·mol$^{-1}$. The heat of formation at 298 K for $K_2Si_4O_9$ (wadeite-type phase) was obtained by subtracting $\Delta H_{298}$ for $K_2Si_4O_9$ (glass from wadeite-type phase), 51.0 ± 1.8 kJ·mol$^{-1}$, from the $\Delta H_{f,298}$ of the glass, −290.0 ± 1.8 kJ·mol$^{-1}$ (Kracek et al., 1953). $\Delta S_{298}$ for the reaction estimated from standard entropies at 298 K (Table 5) is −144.6 ± 4.3 J·mol$^{-1}$·K$^{-1}$. The molar volumes, thermal expansivities, bulk moduli, and their pressure derivatives needed for evaluation of $\Delta V_{T,P}$ are given in Table 6. The phase boundary for the breakdown of K-feldspar was calculated in two ways, first by assuming that $\Delta H$ and $\Delta S$ are constant as a function of temperature and then by incorporating the heat-capacity data (Table 6). The two boundaries are essentially indistinguishable and are shown as a single curve in Figure 6. The slope of the K-feldspar breakdown calculated from the Clausius-Clapeyron relation, $dP/dT = \Delta S/\Delta V$, is 0.003 GPa·K$^{-1}$. To date, there

TABLE 6. Volume, thermal expansion, bulk modulus, and heat-capacity data

| | | $\alpha = \alpha_0 + \alpha_1 \cdot (T - 298)$ (K$^{-1}$) | | | | $C_P = a + bT + cT^{-2} + dT^{-1/2} + eT^2$ (J·K$^{-1}$·mol$^{-1}$) | | | | |
|---|---|---|---|---|---|---|---|---|---|---|
| Phase* | $V^0_{298}$ (cm$^3$·mol$^{-1}$) | $\alpha_0 \times 10^5$ | $\alpha_1 \times 10^8$ | $K$ (GPa) | $K'$ | $a$ | $b \times 10^3$ | $c \times 10^{-5}$ | $d$ | $e \times 10^{-5}$ |
| $KAlSi_3O_8$ (sanidine) | 109.050 | 0.735 | 2.1 | 54.7 | (4)** | 693.534 | −171.740 | 34.631 | −8307.384 | 4.922 |
| $Al_2SiO_5$ (kyanite) | 44.090 | 1.371 | 2.4 | 264.5 | (4)** | 436.600 | −135.791 | — | −4803.849 | 4.725 |
| $SiO_2$ (coesite) | 20.641 | 0.744 | 0.44 | 96.0 | 8.4 | 233.117 | −77.781 | 26.043 | −3376.106 | 1.924 |
| $K_2Si_4O_9$ (wadeite-type) | 108.442 | 2.950 | 0 | 90.0 | (4)** | 749.734 | −155.970 | 19.490 | −8636.597 | 3.692 |
| $K_2Si_4O_9$ (sheet-type) | 143.091 | 2.950 | 0 | 40.0 | (4)** | — | — | — | — | — |

* Sanidine: volume from Kroll and Ribbe (1983); thermal expansion and compressibility of microcline assumed from Kieffer (1980); $C_P$ data from Robie et al. (1978). Kyanite: volume and thermal expansion from Winter and Ghose (1979); compressibility data from Brace et al. (1969); $C_P$ data from Robie et al. (1978). Coesite: volume, thermal expansion, and compressibility data from Akaogi and Navrotsky (1984); $C_P$ data from Robie et al. (1978). Wadeite-type: volume from Swanson and Prewitt (1983); thermal expansion from Swanson and Prewitt (1986); compressibility from Ross, Swanson, and Prewitt (unpub.); $C_P$ data from vibrational calculations in this study. Sheet-type: volume from Schweinsberg and Liebau (1974); thermal expansion assumed to be greaater than or equal to that of wadeite-type phase; compressibility of muscovite used.
** Bulk-moduli pressure derivatives of 4 assumed.

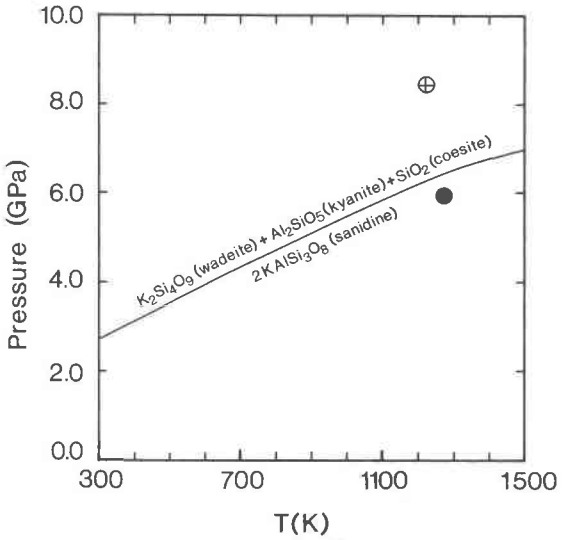


Fig. 6. Calculated phase boundary for breakdown of K-feldspar to $K_2Si_4O_9$ (wadeite-type), $Al_2SiO_5$ (kyanite), and $SiO_2$ (coesite). Data points represent synthesis runs of Seki and Kennedy (1964) (feldspar persists, solid symbol) and Kinomura et al. (1975) (wadeite-type phase, coesite, and kyanite formed, open symbol).

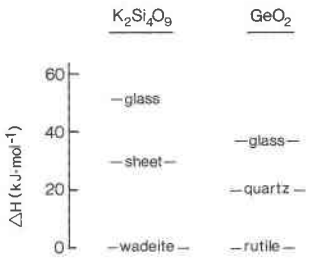


Fig. 7. Schematic "energy-level diagram" for $K_2Si_4O_9$ and $GeO_2$ phases. Data for $K_2Si_4O_9$ from this work, for $GeO_2$ from Navrotsky (1971). In each case, the zero of energy is taken as the phase of lowest enthalpy.

have been no thorough phase-equilibrium studies of the K-feldspar breakdown with pressure. Seki and Kennedy (1964) found that K-feldspar appears stable at 1273 K and 6 GPa. Note there is a discrepancy between abstract and text in Seki and Kennedy's (1964) article, namely, their synthesis run is also listed as 1573 K, 6 GPa. However, using this other value does not change any conclusions. Kinomura et al. (1975) subjected K-feldspar to 1223 K and 8.5 GPa and found it decomposed into a mixture of the wadeite-type phase, kyanite, and coesite. Both of these studies are consistent with the predicted phase boundary (Fig. 6).

## Conclusions

The striking features of the calorimetric results may be summarized by looking at the relative energetic stabilities of $K_2Si_4O_9$ phases on a "energy-level" diagram (Fig. 7) in which the phases are shown in the order of their enthalpies relative to the wadeite-type phase. The energetic differences indicate that a phase with some Si in octahedral coordination ($^{VI}$Si), as in the wadeite-type phase, is not always more costly in terms of energy than a phase with all Si in tetrahedral coordination ($^{IV}$Si), as in the sheet-type phase or the glass. This observation is an exception to the general rule, as recently stated by Liebau (1985, p. 15), that under ordinary conditions for a given composition, the phase containing Si in octahedral coordination should be energetically less favorable than the one with tetrahedrally coordinated Si.

The relative stability of the $K_2Si_4O_9$ polymorphs is somewhat analogous to that observed for $GeO_2$ phases (Fig. 6; Navrotsky, 1971). The low-temperature polymorph of $GeO_2$ has the rutile structure with all $^{VI}$Ge. This transforms with increasing temperature to a polymorph with the $\beta$-quartz structure with all $^{IV}$Ge and then to the liquid with all $^{IV}$Ge. Thus, in this case, $^{VI}$Ge is energetically more stable than $^{IV}$Ge. In the silicates, however, this observed relative stability of $^{VI}$Si in the wadeite-type phase is surprising because of the generally high energy of that change in coordination in other systems, e.g., for $SiO_2$ (quartz → stishovite) $\Delta H_{298} = 51.9$ kJ·mol$^{-1}$ (Akaogi and Navrotsky, 1984) and for $MgSiO_3$ (pyroxene → ilmenite-type structure) $\Delta H = 71.8$ kJ·mol$^{-1}$ (Ito and Navrotsky, 1985).

To rationalize the observed stability, we first note that there is no inherent reason why $^{VI}$Si should be absolutely unstable at low $T$ and $P$. This was concluded by Gibbs (1982) based on ab initio molecular orbital calculations and is supported by the stable occurrence of $^{VI}$Si in molecular crystals (e.g., Flynn and Boer, 1969; Adams et al., 1979) as well as in some low-pressure silicates such as thaumasite $Ca_3Si(OH)_6SO_4CO_3 \cdot 12H_2O$ (Edge and Taylor, 1971) and polymorphs of $SiP_2O_7$ (Tillmans et al., 1973; Bissert and Liebau, 1970; Liebau and Hesse, 1971). However, special local bonding conditions exist in these instances. The Si atoms are associated across their bonded oxygens with strongly bonding atoms, H in the case of thaumasite and tetrahedrally coordinated P in $SiP_2O_7$. In these cases, simple bond-strength arguments have been used to show that $^{VI}$Si is stabilized over $^{IV}$Si to bring the classical Pauling bond-strength sum to the oxygen ($p_O$) down to a value in better agreement with the saturation value of 2.0 (Shannon et al., 1975). If the Si atoms were in fourfold coordination, the bonding to the oxygens would be oversaturated and thus presumably energetically unstable. However, this type of simple bonding argument does not apply to the $K_2Si_4O_9$ phases. The maximum $p_O$ in the low-temperature sheet structure (Schweinsburg and Liebau, 1974) is ~2.2, which is not particularly oversaturated and not any greater than the values of $p_O$ in the wadeite-type structure, namely 1.9 and 2.2 (Swanson and Prewitt, 1983).

The question then becomes one of relative stability among different possible structures with $^{VI}$Si and $^{IV}$Si. We suggest that an understanding of the relative stabilities of these $K_2Si_4O_9$ polymorphs lies in the structure of the sheet-type phase. The oxygen to tetrahedral atom ratio of 2.25

lies below the average value for a sheet silicate of ~2.5 and above that for a framework silicate of ~2.0. Therefore, it may be impossible to simultaneously satisfy the bonding requirements of all the oxygens. This less-than-optimum bonding is supported by a minimum $p_O$ value for the nonbridging oxygens in the low-temperature sheet structure of ~1.5, with a corresponding extremely short tetrahedral Si–O bond length of 1.545 Å, and also by the extremely broad range of tetrahedral bond lengths (1.55–1.66 Å).

In comparison, the wadeite-type structure might be best viewed as a framework, although, under the usual classification schemes, it is a cyclosilicate. If we ignore cation coordination numbers and simply consider Si and oxygen atoms, every oxygen is bonded to two Si with $p_O$ near the stable saturation value of 2.0, as in a framework silicate (see Liebau, 1985, p. 92).

In other words, the unique condensation of silicate tetrahedra that forms the $[Si_8O_{18}]$ sheet may not be a very energetically efficient way of bonding the Si and O atoms, even relative to a condensation of silicate octahedra and tetrahedra. The fact that a stability field for the sheet silicate exists at all is probably by virtue of its extremely large entropy. The relative energetic instability (with respect to the wadeite-type structure) and the high entropy suggest that the sheet structures are basically entropy-stabilized phases. In addition to high vibrational entropy, structural disorder occurs (Schweinsberg and Liebau, 1974; Durovic, 1974), which would also contribute to the entropy. The low energetic stability and large volume also limit the stability field of the sheet-type phases at high temperature and moderate pressure as indicated by disproportionation to $K_2Si_2O_5 + 2SiO_2$ (quartz) or incongruent melting (Goranson and Kracek, 1932). It is interesting to note that no compounds of $A_2Si_4O_9$ (A = alkali) stoichiometry have been reported for Li or Na and that the structures of the Rb and Cs tetrasilicate are apparently quite different from the structures of K tetrasilicate on the basis of their powder diffraction patterns (Alekseeva, 1966).

## Acknowledgments

We gratefully acknowledge D. K. Swanson (SUNY Stony Brook) for providing a sample of the high-pressure polymorph. This work was supported by NSF Grants DMR 8106027 and DMR 8521562. P. McMillan acknowledges support from NSF Grant EAR 8407105. We thank J. E. Dickinson for kindly sending a Raman spectrum of bulk $K_2Si_4O_9$ glass and allowing us to reproduce it here. We acknowledge J. E. Dickinson and an anonymous reviewer for their careful reviews.

## References

Adams, T., Debaerdemacker, T., and Thewalt, U. (1979) Complexes of six-coordinate silicon. Collected Abstracts, 5th European Crystallographic Meeting, Copenhagen, 32S.

Akogi, M., and Navrotsky, A. (1984) The quartz-coesite-stishovite transformations: New calorimetric measurements and calculation of phase diagrams. Physics of the Earth and Planetary Interiors, 36, 124–134.

Alekseeva, Z.D. (1966) The $Cs_2O$-$SiO_2$ system. Russian Journal of Inorganic Chemistry, 11, 626–629.

Anderson, O.L. (1966) The use of ultrasonic measurements under modest pressure to estimate compression at high pressure. Journal of Physics and Chemistry of Solids, 27, 547–565.

Bissert, G., and Liebau, F. (1970) Die Kristallstruktur von monoklinem Siliziumphosphat $SiP_2O_7$III: Eine phase mit $[SiO_6]$-Oktaedern. Acta Crystallographica, B26, 233–240.

Brace, W.F., Schol, C.H., and La Mori, P.N. (1969) Isothermal compressibility of kyanite, andalusite, and sillimanite from synthetic aggregates. Journal of Geophysical Research, 74, 2089–2098.

Brawer, S.A., and White, W.B. (1975) Raman spectroscopic investigation of silicate glasses. I. The binary alkali silicates. Journal of Chemical Physics, 63, 2421–2432.

Conjeaud, M., and Boyer, H. (1980) Some possibilities of Raman microprobe in cement chemistry. Cement and Concrete Research, 10, 61–70.

Dickinson, J.E., Jr., and Scarfe, C.M. (1985) Pressure-induced structural changes in $K_2Si_4O_9$ silicate melt. EOS, 66, 395.

Domine, F., and Piriou, B. (1986) Raman spectroscopic study of the $SiO_2$-$Al_2O_3$-$K_2O$ vitreous system: Distribution of silicon second neighbors. American Mineralogist, 71, 38–50.

Durovic, S. (1974) Die Kristallstruktur des $K_4[Si_8O_{18}]$: Eine desymmetrisierter OD Struktur. Acta Crystallographica, B30, 2214–2217.

Edge, R.A., and Taylor, H.F.W. (1971) Crystal structure of thaumasite, $Ca_3Si(OH)_6 \cdot 12H_2O(SO_4)(CO_3)$. Acta Crystallographica, B27, 594–601.

Eliezer, N., Howald, R.A., Marinkovic, M., and Eliezer, I. (1978) Vapor pressure measurements, thermodynamic parameters and phase diagram for the system potassium-silicon oxide at high temperatures. Journal of Physical Chemistry, 82, 1021–1026.

Flynn, J.J., and Boer, F.P. (1969) Structural studies of hexacoordinate silicon. Tris(*o*-phenylenedioxy)siliconate. Journal of the American Chemical Society, 91, 5756–5761.

Gibbs, G.V. (1982) Molecules as models for bonding in silicates. American Mineralogist, 67, 421–450.

Goranson, R.W., and Kracek, F.C. (1932) An experimental investigation of phase relations of $K_2Si_4O_9$ under pressure. Journal of Physical Chemistry, 36, 913–926.

Ito, E., and Navrotsky, A. (1985) $MgSiO_3$ ilmenite: Calorimetry, phase-equilibria, and decomposition at atmospheric pressure. American Mineralogist, 70, 1020–1026.

Kieffer, S.W. (1979a) Thermodynamics and lattice vibrations of minerals: 1. Mineral heat capacities and their relationships to simple lattice vibrational modes. Reviews of Geophysics and Space Physics, 17, 1–19.

——— (1979b) Thermodynamics and lattice vibrations of minerals: 2. Vibrational characteristics of silicates. Reviews of Geophysics and Space Physics, 17, 20–34.

——— (1979c) Thermodynamics and lattice vibrations of minerals: 3. Lattice dynamics and an approximation for minerals with application to simple substances and framework silicates. Reviews of Geophysics and Space Physics, 17, 35–58.

——— (1980) Thermodynamics and lattice vibrations of minerals: 4. Application to chain and sheet silicates and orthosilicates. Reviews of Geophysics and Space Physics, 18, 862–886.

Kinomura, N., Kume, S., and Koizumi, M. (1975) Synthesis of $K_2SiSi_3O_9$ with silicon in 4- and 6-coordination. Mineralogical Magazine, 40, 401–404.

Kracek, F.C., Bowen, N.L., and Morey, G.W. (1929) The system potassium metasilicate-silica. Journal of Physical Chemistry, 33, 1857–1879.

Kracek, F.C., Neuvonen, K.J., Burley, G., and Gordon, R.J. (1953) Contributions of thermochemical and X-ray data to the problem of mineral stability. Annual Report of the Director of the Geophysical Laboratory, Carnegie Institution of Washington, 69–73.

Kroll, M., and Ribbe, P.H. (1983) Lattice parameters, composition, and Al, Si order in feldspars. Mineralogical Society of America Reviews in Mineralogy, 2 (2nd edition), 57–98.

Lazarev, A.N. (1962) Vibrational spectra of silicates. IV. Interpretation of the spectra of silicates and germanates with ring anions. Optics and Spectroscopy, 12, 28–31.

——— (1972) Vibrational spectra and structure of silicates. Consultants Bureau, New York.

Liebau, F. (1985) Structural chemistry of silicates. Springer-Verlag, Berlin.

Liebau, F., and Hesse, K.-F. (1971) Die Kristallstruktur einer zweiten

monoklinen Siliciumdiphosphatphase, $SiP_2O_7$ A IV, mit oktaedrisch koordiniertem Silicium. Zeitschrift für Kristallographie, 133, 213–224.

Matson, D.W., Sharma, S.K. and Philpotts, J.A. (1983) The structure of high-silica alkali-silicate glasses—A Raman spectroscopic investigation. Journal of Non-Crystalline Solids, 58, 323–352.

——— (1986) Raman spectra of some tectosilicates and of glasses along the orthoclase-anorthite and nepheline-anorthite joins. American Mineralogist, 71, 694–704.

McMillan, P. (1984) Structural studies of silicate glasses and melts—Applications and limitations of Raman spectroscopy. American Mineralogist, 69, 622–644.

Moenke, H.H.W. (1975) Silica, the three-dimensional silicates, borosilicates and beryllium silicates. In V.C. Farmer, Ed., The infrared spectra of minerals, p. 365–382. Mineralogical Society, London.

Mysen, B.O., Virgo, D., and Seifert, F.A. (1982) The structure of silicate melts: Implications for chemical and physical properties of natural magma. Reviews of Geophysics and Space Physics, 20, 353–383.

Navrotsky, A. (1971) Enthalpies of transformation among the tetragonal, hexagonal, and glassy modifications of $GeO_2$. Journal of Inorganic and Nuclear Chemistry, 33, 1119–1124.

——— (1977) Progress and new directions in high temperature calorimetry. Physics and Chemistry of Minerals, 2, 89–104.

Navrotsky, A., Pintchovski, F.S., and Akimoto, S. (1979) Calorimetric study of the stability of high pressure phases in the systems CoO-$SiO_2$ and "FeO"-$SiO_2$ and calculation of phase diagrams in MO-$SiO_2$ systems. Physics of the Earth and Planetary Interiors, 19, 275–292.

Richet, P., and Bottinga, Y. (1980) Heat capacity of liquid silicates: New measurements on $NaAlSi_3O_8$ and $K_2Si_4O_9$. Geochemical et Cosmochimica Acta, 44, 1535–1541.

Robie, R.A., Hemingway, B.S., and Fisher, J.R. (1978) Thermodynamic properties of minerals and related substances at 298.15 K and 1 bar ($10^5$ pascals) pressure, and at higher temperatures. U.S. Geological Survey Bulletin 1452.

Ross, N.L., Akaogi, M., Navrotsky, A., Susaki, J., and McMillan, P. (1986) Phase transitions among the $CaGeO_2$ polymorphs (wollastonite, garnet, and perovskite structure): Studies by high pressure synthesis, high temperature calorimetry, and vibrational spectroscopy and calculations. Journal of Geophysical Research, 91, 4685–4696.

Rutstein, M.S., and White, W.B. (1971) Vibrational spectra of high-calcium pyroxenes and pyroxenoids. American Mineralogist, 56, 877–887.

Schweinsberg, H., and Liebau, F. (1972) Darstellung und kristallographische Daten von $K_2Si_2O_5$, $KHSi_2O_5I$ und $K_2Si_4O_9$. Zeitschrift für anorganische und allgemeine Chemie, 387, 241–251.

——— (1974) Die Kristallstruktur des $K_4[Si_8O_{18}]$: Ein neuer Silikat-Schichttyp. Acta Crystallographica, B30, 2206–2217.

Seki, Y., and Kennedy, G.C. (1964) The breakdown of potassium feldspar, $KAlSi_3O_8$, at high temperatures and high pressures. American Mineralogist, 49, 1688–1706.

Shannon, R.D., Chenavas, J., and Joubert, J.C. (1975) Bond strength considerations applied to cation coordination in normaland high-pressure oxides. Journal of Solid State Chemistry, 12, 16–30.

Sharma, S.K., Mammone, J.F., and Nichol, M.F. (1981) Raman investigation of ring configurations in vitreous silica. Nature, 292, 140–141.

Swanson, D.K., and Prewitt, C.T. (1983) The crystal structure of $K_2Si^{VI}Si_3^{IV}O_9$. American Mineralogist, 68, 581–585.

——— (1986) Anharmonic thermal motion in $K_2Si^{VI}Si_3^{IV}O_9$ (abs.) EOS, 67, 369.

Tillmans, E., Gerbert, W., and Baur, W.H. (1973) Computer simulation of crystal structures applied to the solution of the superstructure of cubic silicon diphosphate. Journal of Solid State Chemistry, 7, 69–84.

Verweij, H., and Konijnendijk, W.L. (1976) Structural units in $K_2O$-PbO-$SiO_2$ glasses by Raman spectroscopy. American Ceramic Society Journal, 59, 517–521.

Weng, K., Xu, J., Mao, H.-K., and Bell, P.M. (1983) Preliminary Fourier-transform infrared spectral data on the $SiO_6^{8-}$ octahedral group in silicate-perovskite. Carnegie Institution of Washington Year Book 82, 355–356.

Williams, Q., Jeanloz, R., and McMillan, P. (1987) The vibrational spectrum of $MgSiO_3$-perovskite: Zero pressure Raman and mid-infrared spectra to 27 GPa. Journal of Geophysical Research, in press.

Winter, J.K., and Ghose, S. (1979) Thermal expansion and high-temperature crystal chemistry of the $Al_2SiO_5$ polymorphs. American Mineralogist, 64, 573–586.

Manuscript received November 10, 1986
Manuscript accepted May 26, 1987